



Fourth Exception in the Calculation of Relic Abundances

Raffaele Tito D’Agnolo*

*Theoretical Particle Physics Laboratory, Institute of Physics, EPFL, Route Cantonale, 1015 Lausanne, Switzerland
and Institute for Advanced Study, Princeton, New Jersey 08540, USA*

Duccio Pappadopulo[†] and Joshua T. Ruderman[‡]

Center for Cosmology and Particle Physics, Department of Physics, New York University, New York, New York 10003, USA

(Received 1 June 2017; revised manuscript received 10 July 2017; published 8 August 2017)

We propose that the dark matter abundance is set by the decoupling of inelastic scattering instead of annihilations. This cospattering mechanism is generically realized if dark matter scatters against states of comparable mass from the thermal bath. Cospattering points to dark matter that is exponentially lighter than the weak scale and has a suppressed annihilation rate, avoiding stringent constraints from indirect detection. Dark matter upscatters into states whose late decays can lead to observable distortions to the blackbody spectrum of the cosmic microwave background.

DOI: [10.1103/PhysRevLett.119.061102](https://doi.org/10.1103/PhysRevLett.119.061102)

Introduction.—Dark matter (DM) constitutes most of the matter in our Universe, but its origin is unknown. One of the most attractive possibilities is that DM starts in thermal equilibrium in the early Universe, and its abundance is set once its annihilations become slower than the expansion rate. This framework is insensitive to initial conditions and has the further appeal of tying the DM abundance to its (potentially observable) interactions.

The most widely considered possibility is that 2-to-2 annihilations to standard model (SM) particles set the DM relic density. This is known as the weakly interacting massive particle (WIMP) paradigm [1–4] and points to DM particles with weak scale masses and cross sections. This theoretical framework has had considerable impact shaping experimental searches for DM.

However it has long been appreciated that simple variations to the cosmology of thermal relics can have dramatic consequences. In a seminal paper, Ref. [5] enumerates three “exceptions” to thermal relic cosmology: (1) mutual annihilations of multiple species (coannihilations), (2) annihilations into heavier states (forbidden channels), and (3) annihilations near a pole in the cross section. These exceptions lead to phenomenology that can differ significantly from standard WIMPs (see for example Refs. [6–14]), while sharing their appealing theoretical features.

In this letter, we introduce a fourth exception. Like Ref. [5], we assume DM begins in thermal equilibrium, has its number diluted through 2-to-2 annihilations, and has a temperature that tracks the photon temperature (for studies that relax at least one of these assumptions, see for example Refs. [15–28]). We consider the presence of two states charged under the symmetry that stabilizes DM: χ and ψ , where $m_\chi < m_\psi$ and χ is DM. We assume that χ annihilations are suppressed, and two processes are active: (1) χ/ψ interchange: $\chi\phi \leftrightarrow \psi\phi$ (left of Fig. 1), (2) ψ annihilations: $\psi\psi \rightarrow \phi\phi$ (right of Fig. 1), where ϕ is an

unstable state from the thermal bath. When both processes are in equilibrium, DM number is diluted from $\chi \rightarrow \psi$ scattering followed by $\psi\psi$ annihilations. This picture can be generalized to include multiple states ψ_i, ϕ_j .

In the coannihilation phase, it is assumed that process (2) decouples before process (1), such that the DM abundance is set by the freeze-out of annihilations [5]. We introduce the phase, cospattering, where process (1) shuts off before process (2), such that the DM abundance is determined by the freeze-out of inelastic scattering. As we see, cospattering is generically realized in a large class of models if DM scatters against massive states, $m_\phi \sim m_\chi$. We note that a similar process was considered within supersymmetry for the special case of an ultralight gluino with a sub-GeV mass, where χ, ψ , and ϕ were identified with the photino, R -hadron, and pion [29,30].

Cospattering leads to unique phenomenology. As we describe below, the DM abundance has a different parametric form than the WIMP. In order to reproduce the observed

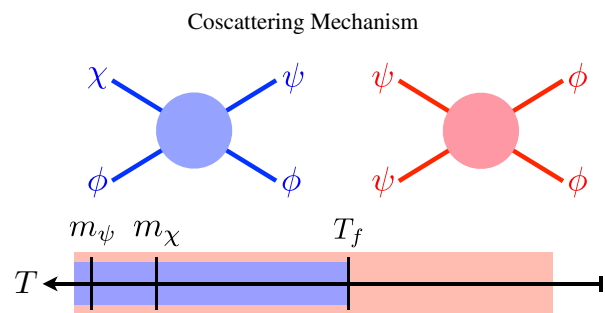


FIG. 1. An illustration of the cospattering mechanism for DM freeze-out. If both diagrams are active, the abundance of DM, χ , decreases through inelastic scattering, $\chi\phi \rightarrow \psi\phi$, followed by annihilations, $\psi\psi \rightarrow \phi\phi$. Cospattering corresponds to the phase where scattering freezes out before annihilations, setting the DM abundance.

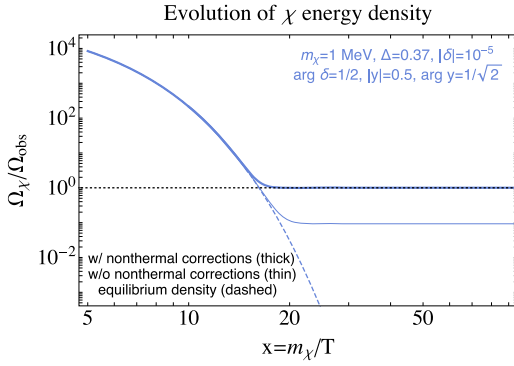


FIG. 2. Evolution of χ energy density for coscattering. The thin blue line represents the solution of Eq. (2) where χ is assumed to be in kinetic equilibrium, while the thick blue line is the solution of the full Boltzmann equation [Eq. (7)]. The dashed blue line represents the equilibrium number density.

abundance, the DM mass is generically much lighter than the weak scale. The DM self-annihilation rate can be arbitrarily small, evading stringent limits from the cosmic microwave background (CMB) [31–33]. Although χ constitutes DM, there is also a relic population of ψ that decays to χ at late times. These ψ decays can produce observable distortions to the blackbody spectrum of the CMB.

The rest of this Letter is organized as follows. We begin by analyzing the relic density of DM produced by coscattering. We then discuss nontrivial thermal corrections to the abundance, which are further elaborated in Supplemental Material [34]. Finally, we determine the relic density and experimental constraints in an example model.

Relic abundance.—As above, we consider DM, χ , and a heavier state, ψ , that are both charged under the DM stabilizing symmetry. DM can upscatter into ψ through the coscattering process: $\chi\phi \rightarrow \psi\phi$, where ϕ is an unstable state from the thermal bath.

If χ and ψ are in kinetic equilibrium (we relax this assumption in the next section), the evolution of their number densities, $n_{\chi,\psi}$, are determined by the solution to the following system of Boltzmann equations [5,13,30,35],

$$\begin{aligned} \dot{n}_i + 3Hn_i = & -\sum_j \left[n_{\phi}^{\text{eq}} \langle \sigma_{i \rightarrow j} v \rangle \left(n_i - n_i^{\text{eq}} \frac{n_j}{n_j^{\text{eq}}} \right) \right. \\ & \left. + \langle \sigma_{ij} v \rangle (n_i n_j - n_i^{\text{eq}} n_j^{\text{eq}}) \right], \end{aligned} \quad (1)$$

where $i, j = (\psi, \chi)$, n_i^{eq} denotes the equilibrium Boltzmann distribution, H is the Hubble parameter, and we have assumed that ϕ remains in equilibrium. The first line corresponds to coscattering, $\chi\phi \leftrightarrow \psi\phi$, while the second line corresponds to coannihilations, $\psi\psi, \psi\chi, \chi\chi \rightarrow \phi\phi$. We have assumed that two-body decays, $\psi \rightarrow \chi\phi$, are kinematically forbidden: $m_{\phi} > m_{\psi} - m_{\chi}$. When two-body decays are active, they typically equilibrate ψ and χ , and then the coscattering diagram does not determine the relic density. The absence of decays in coscattering is an

important difference compared to the light gluino scenario of Refs. [29,30], where decays are active.

Coscattering is realized when the following conditions are met: (1) $\psi\psi \rightarrow \phi\phi$ is in equilibrium, (2) $\chi\chi, \chi\psi \rightarrow \phi\phi$ can be neglected, and (3) two-body decays are kinematically forbidden, $m_{\phi} > m_{\psi} - m_{\chi}$. In this limit, $n_{\psi} = n_{\psi}^{\text{eq}}$, and the Boltzmann equations simplify,

$$\dot{n}_{\chi} + 3Hn_{\chi} = -n_{\phi}^{\text{eq}} \langle \sigma_{\chi \rightarrow \psi} v \rangle (n_{\chi} - n_{\chi}^{\text{eq}}). \quad (2)$$

The solution to Eq. (2) is approximated by taking the DM abundance to be constant after $\chi \leftrightarrow \psi$ decouples, which occurs when

$$n_{\phi}^{\text{eq}} \langle \sigma_{\chi \rightarrow \psi} v \rangle \approx pH, \quad (3)$$

where we find that $p \sim 20$ replicates numerical solutions to Eq. (2).

The $\chi \rightarrow \psi$ scattering is endothermic because $m_{\chi} < m_{\psi}$. The thermally averaged cross section, $\langle \sigma_{\chi \rightarrow \psi} v \rangle$, is exponentially suppressed in the limit $T \ll m_{\psi} - m_{\chi}$. The exponential dependence can be derived by using detailed balance to write the $\chi \rightarrow \psi$ cross section as a function of the cross section for the inverse process

$$\langle \sigma_{\chi \rightarrow \psi} v \rangle = \frac{n_{\psi}^{\text{eq}}}{n_{\chi}^{\text{eq}}} \langle \sigma_{\psi \rightarrow \chi} v \rangle \approx \frac{m_{\psi}^{3/2}}{m_{\chi}^{3/2}} e^{-x\Delta} \langle \sigma_{\psi \rightarrow \chi} v \rangle, \quad (4)$$

where $x \equiv m_{\chi}/T$, $\Delta \equiv (m_{\psi} - m_{\chi})/m_{\chi}$, and $\langle \sigma_{\psi \rightarrow \chi} v \rangle$ is not exponentially suppressed at low temperatures because $\psi \rightarrow \chi$ is exothermic.

Using Eq. (4) to solve Eq. (3), we find that freeze-out occurs at temperature

$$(r + \Delta)x_f = 21 + \log \left(\frac{(r + r\Delta)^{3/2} m_{\chi} \sigma_{\text{inv}}}{p \sqrt{g_*} \text{GeV} \times \text{pb}} \right) + \log \sqrt{x_f}, \quad (5)$$

where $\sigma_{\text{inv}} \equiv \langle \sigma_{\psi \rightarrow \chi} v \rangle$, $r \equiv m_{\phi}/m_{\chi}$, and g_* correspond to the number of relativistic degrees of freedom at freeze-out.

Using Eq. (5), we can estimate the relic density,

$$\frac{\Omega_{\chi}}{\Omega_{\text{DM}}} \approx \frac{0.6 \text{ pb}}{\sigma_{\text{inv}}} \frac{p x_f e^{x_f(r+\Delta-1)}}{\sqrt{g_*} r^{3/2} (1+\Delta)^{3/2}}. \quad (6)$$

Unlike a WIMP, which requires a weak scale annihilation cross section of order 1 pb, the abundance (freeze-out temperature) has an exponential (nonlogarithmic) sensitivity on the spectrum.

For $r + \Delta > 1$ (i.e., $m_{\phi} + m_{\psi} > 2m_{\chi}$), σ_{inv} should be exponentially larger than the weak scale in order to reproduce the observed relic density, $\Omega_{\chi} h^2 \approx 0.12$ [31]. This points to DM that is exponentially lighter than the weak scale. In the opposite limit, $r + \Delta < 1$, DM cannot be much heavier than the weak scale without violating the requirement that $\psi\psi$ annihilations respect perturbativity

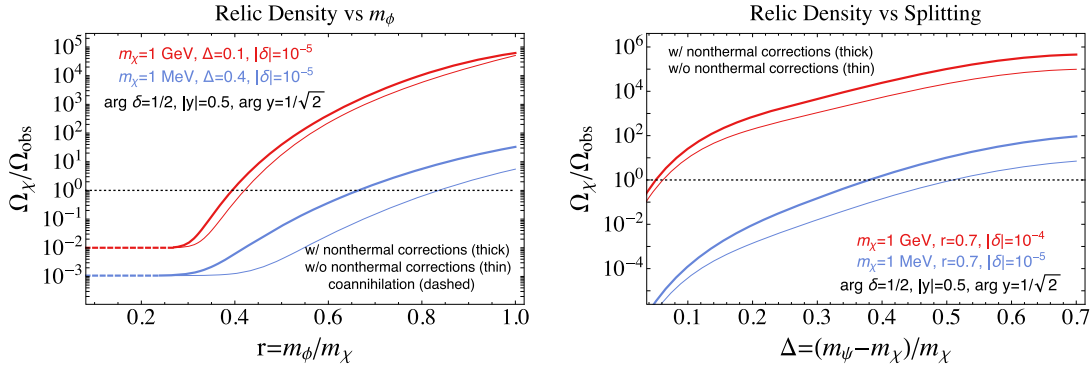


FIG. 3. The left side shows the dark matter relic density normalized to its measured value, versus m_ϕ/m_χ . The plot shows the transition between the coannihilation and cospattering phases, where Ω_χ depends exponentially on m_ϕ . The right side shows the relic density normalized to its measured value, versus Δ . In both panels the thin solid curves represent the result of the calculation performed assuming kinetic equilibrium for χ , while the thick solid lines are the solution of the full Boltzmann equation [Eq. (7)].

and remain in equilibrium until the cospattering process decouples. It is straightforward to generalize our analysis to multiple states ψ_i, ϕ_j .

Departure from kinetic equilibrium.—For conventional WIMPs, DM experiences rapid elastic scattering against the thermal bath while annihilations decouple. Therefore, kinetic decoupling (the departure from Maxwell-Boltzmann phase space distribution) occurs long after chemical decoupling (the freeze-out of number changing interactions); see for example Refs. [36–38]. For cospattering, elastic scattering, $\chi\phi \rightarrow \chi\phi$, generically decouples before inelastic scattering, $\chi\phi \rightarrow \psi\phi$, because of the small coupling of χ to the thermal bath. Therefore, $\chi\phi \rightarrow \psi\phi$ is responsible for maintaining both chemical and kinetic equilibrium, and its freeze-out brings simultaneous chemical and kinetic decoupling. This is an important difference between cospattering and WIMPs and it means that Eq. (2) is not strictly applicable, as it assumes an equilibrium phase space distribution for χ .

In order to correctly treat the departure from kinetic equilibrium, we must solve the full (unintegrated) Boltzmann equation for the time dependence of the momentum space distribution of χ , $f_\chi(p, t)$,

$$\left(\frac{\partial}{\partial t} - \mathbf{H}\mathbf{p} \cdot \nabla_{\mathbf{p}}\right) f_\chi(p, t) = \frac{1}{E} C[f_\chi], \quad (7)$$

where $C[f_\chi]$ is the collision operator induced by the cospattering reaction $\chi\phi \rightarrow \psi\phi$. $C[f_\chi]$ is a linear function of f_χ . Therefore, Eq. (7) is a solvable first-order linear partial differential equation. We now provide a qualitative sketch of its solution, and we provide more details in Supplemental Material [34]. We find that lower momentum modes of χ decouple earlier than higher momentum modes. This is because the cospattering process is endothermic and χ modes with smaller kinetic energy can only interact with energetic ϕ modes from the tail of the Boltzmann distribution with suppressed number density. Because low

momentum modes are more abundant, the final relic abundance of χ is enhanced relative to the solution of Eq. (2). The size of this thermal correction grows with Δ , which controls the degree of endothermicity of cospattering. While Eq. (6) correctly captures the abundance at the order-of-magnitude level, thermal corrections arising from Eq. (7) are required for a precise calculation of the abundance (see for example Figs. 2 and 3 to be discussed below), and are included in our numerical results that follow.

An example dark sector.—Cospattering is naturally realized within the framework of hidden sector DM [15,18,19,39–46], where χ, ψ , and ϕ are neutral under the SM gauge group. We take χ, ψ to be Majorana fermions, and ϕ to be a real scalar, with the following interactions:

$$\mathcal{L} \supset -\frac{m_\chi}{2}\chi^2 - \frac{m_\psi}{2}\psi^2 - \delta m\chi\psi - \frac{y}{2}\phi\psi^2 + \text{H.c.} \quad (8)$$

Notice that ψ is active, with Yukawa coupling to ϕ , while χ is sterile. There is a mass mixing, δm , whose strength is determined by the dimensionless parameter $\delta \equiv \delta m/m_\chi$. We focus on the small mixing limit, $\delta \ll 1$, where ψ, χ are approximately mass eigenstates, $n_1 \approx \chi$ and $n_2 \approx \psi$. Without loss of generality, we take $m_{\chi,\psi}$ to be real and allow generic phases in y and δm in order to avoid p -wave suppression of the relevant processes. Note that the structure of the interaction of χ in Eq. (8) is a natural consequence of a softly broken chiral symmetry.

The annihilation $\psi\psi \rightarrow \phi\phi$ is unsuppressed while $\psi\chi$ and $\chi\chi$ annihilations are suppressed by δ^2 and δ^4 , respectively. The inverse cospattering cross section, $\psi\phi \rightarrow \chi\phi$, which determines the relic density [σ_{inv} in Eq. (6)], is $\langle \sigma_{\psi \rightarrow \chi} v \rangle \approx f(r)\sqrt{\Delta}(y^4\delta^2/2\pi m_\chi^2)$, where $f(r) \equiv (r^2 + r + 2)^2/(\sqrt{2}(r-2)^2 r^{9/2}(r+1)^{7/2})$. For simplicity, we derive this expression by assuming real δm and y and taking the limit $\delta \ll \Delta \ll 1$.

Figure 2 shows the χ energy density as a function of x . We see that Eq. (2) underestimates the χ abundance compared to the solution of Eq. (7). For the parameter

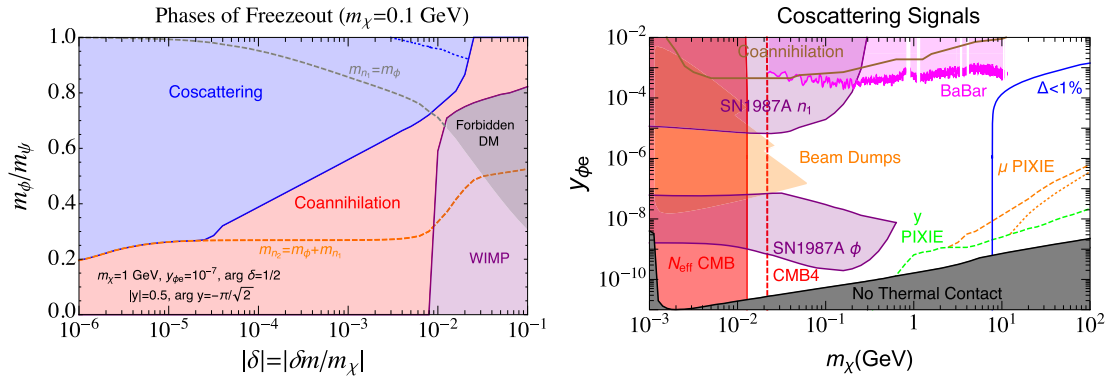


FIG. 4. The left side shows how the different phases of freeze-out depend on (m_ϕ, δ) . Below the dotted blue line, in the coscattering region, elastic scattering, $\chi\phi \rightarrow \chi\phi$, decouples before the coscattering diagram, and thermal effects are important. The right side summarizes the phenomenology of the model for a mediator ϕ coupling to electrons. Supernova cooling constrains both the direct production of ϕ and that of dark matter n_1 , while we find that $n_2 \approx \psi$ is always trapped inside the star. The other constraints are described in the main body of the text. Dark matter PIXIE corresponds to $\mu < 2.8 \times 10^{-8}$ and $y < 2.4 \times 10^{-9}$ [48,49]. The reach including the expected impact of foregrounds, $\mu < 9.4 \times 10^{-8}$ [50], is shown with a dotted line. The remaining model parameters are set to $|y| = 1$, $|\delta| = 10^{-4}$, $\arg y = -i\pi/\sqrt{2}$, $\arg \delta = 1/2$, and $m_\phi/m_\chi = 0.9$. On both sides, Δ is fixed at each point to reproduce the observed relic density.

choice displayed in Fig. 2, chemical freeze-out of the coscattering process occurs at $x \approx 20$, while elastic scattering, $\chi\phi \rightarrow \chi\phi$, freezes out earlier, $x \approx 10$.

Figure 3 shows how the relic density, Ω_χ , depends on $r \equiv m_\phi/m_\chi$ and $\Delta \equiv (m_\psi - m_\chi)/m_\chi$. The relic density is exponentially sensitive to these quantities [Eq. (6)]. For the chosen parameters, the departure from kinetic equilibrium is always relevant. The right of Fig. 3 shows that thermal corrections from Eq. (7) are enhanced as the splitting Δ increases.

It is clear from the previous discussion and Fig. 3 that coscattering and coannihilations are closely related [47]. By varying parameters, any model with coannihilations also realizes coscattering. The left of Fig. 4 is the phase diagram, which shows the transition from the coscattering to the coannihilation phase as δ and m_ϕ are varied. Coscattering occurs in the region with small mixing, $\delta \ll 1$, and heavy ϕ , $m_\phi \sim m_\psi$. This is because the ratio between the coscattering and $\psi\psi \rightarrow \phi\phi$ rates scales as $\sim \delta^2 n_\phi^{\text{eq}}/n_\psi^{\text{eq}} \sim \delta^2 e^{(m_\psi - m_\phi)/T}$.

For completeness, the left of Fig. 4 also shows the WIMP phase, where the relic density is set by the freeze-out of $\chi\chi \rightarrow \phi\phi$. It is divided into the conventional case, $m_\chi > m_\phi$, and the forbidden regime [5,10], $m_\chi < m_\phi$.

Phenomenology.—So far, we have implicitly assumed that ϕ is part of the thermal bath and can decay to other species. The simplest possibility is that ϕ couples to SM particles, leading to experimental signals. In the following, we assume that ϕ couples to electrons,

$$\mathcal{L} \supset -y_{\phi e} \phi \bar{e} + \text{H.c.} \quad (9)$$

For large enough coupling, $y_{\phi e} \gtrsim 10^{-10}$, the dark sector is in kinetic equilibrium with the SM, implying that the DM temperature tracks the photon temperature. When the coupling becomes too large, $y_{\phi e} \gtrsim 10^{-3}$, dark matter

scattering off electrons, $\chi e^\pm \rightarrow \psi e^\pm$, keeps χ and ψ in equilibrium, bringing the model back into the coannihilation phase. Coscattering is therefore realized for a wide range of couplings: $y_{\phi e} \sim 10^{-(3-10)}$.

The various phenomenological constraints are summarized on the right side of Fig. 4, where we fix $m_\phi/m_\chi = 0.9$. The scalar mediator is constrained by direct production in beam dump experiments [51–54], BABAR [55], and supernovae [56–61]. Since ϕ couples to electrons but not neutrinos, it modifies their relative temperatures after the weak interactions decouple, changing the effective number of neutrinos, N_{eff} [62]. We show the current constraints from Planck [31] and the projected reach of CMB stage-4 experiments [63].

To conclude this section we discuss a characteristic signal of coscattering. In the coscattering regime, the leading decay of ψ is three body, $\psi \rightarrow \chi e^+ e^-$, and ψ is typically long lived,

$$\tau_\psi \approx 1.2 \times 10^8 \text{ s} \left(\frac{10 \text{ GeV}}{m_\psi} \right) \left(\frac{10^{-12}}{y_{e\phi}\delta} \right)^2 \left(\frac{0.01}{\Delta} \right)^3 r^4. \quad (10)$$

These decays can inject energy into CMB photons after the decoupling of double Compton scattering, modifying the blackbody spectrum by producing μ or y distortions [64,65]. Current constraints from FIRAS [66] do not appear in Fig. 4, but the proposed PIXIE mission [49] has the potential to cover significant new parameter space. Spectral distortions are typical of coscattering, beyond this particular model realization, because DM upscatters into a heavier state that generically has a trace relic abundance and long lifetime.

Conclusions.—In this Letter we have introduced the coscattering phase for DM freeze-out. Coscattering is of broader significance than the example model of Eq. (8).

The requirements are (1) mostly sterile DM, χ , with suppressed annihilations, (2) heavier active states, ψ_i , with rapid annihilations, and (3) 2-to-2 scatterings against the thermal bath that initially keep DM in equilibrium with the heavier states until these inelastic scatterings decouple and set the DM relic density. In order to more fully explore the phenomenology of coscattering, it would be interesting to consider more hidden sectors that realize these conditions, and more portals that connect these sectors to the SM.

We thank Francesco D’Eramo for collaboration at an earlier stage. We thank Daniele Alves, Jens Chluba, Rouven Essig, Mariangela Lisanti, Cristina Mondino, Maxim Pospelov, Kris Sigurdson, Tracy Slatyer, and James Wang for helpful discussions. We thank Bertrand Echenard for providing the numerical limit on a resonance decaying to electrons from Ref. [55]. We thank Lawrence Hall for suggesting the name coscattering. R. T. D. is supported by Swiss National Science Foundation Contract No. 200020-169696 and the Sinergia network Grant No. CRSII2-160814. D. P. and J. T. R. are supported by NSF CAREER Grant No. PHY-1554858. R. T. D. and J. T. R. acknowledge the hospitality of the Aspen Center for Physics, which is supported by the NSF Grant No. PHY-1066293. We thank the Institute for Advanced Study for use of computing facilities.

*raffaele.dagnolo@epfl.ch

†duccio.pappadopulo@gmail.com

*ruderman@nyu.edu

- [1] B. W. Lee and S. Weinberg, *Phys. Rev. Lett.* **39**, 165 (1977).
 [2] E. W. Kolb and M. S. Turner, *Front. Phys.* **69**, 1 (1990).
 [3] P. Gondolo and G. Gelmini, *Nucl. Phys.* **B360**, 145 (1991).
 [4] G. Jungman, M. Kamionkowski, and K. Griest, *Phys. Rep.* **267**, 195 (1996).
 [5] K. Griest and D. Seckel, *Phys. Rev. D* **43**, 3191 (1991).
 [6] N. Arkani-Hamed, A. Delgado, and G. F. Giudice, *Nucl. Phys.* **B741**, 108 (2006).
 [7] S. Tulin, H. B. Yu, and K. M. Zurek, *Phys. Rev. D* **87**, 036011 (2013).
 [8] N. Bernal, C. Garcia-Cely, and R. Rosenfeld, *J. Cosmol. Astropart. Phys.* **04** (2015) 012.
 [9] A. Ibarra, A. Pierce, N. R. Shah, and S. Vogl, *Phys. Rev. D* **91**, 095018 (2015).
 [10] R. T. D’Agnolo and J. T. Ruderman, *Phys. Rev. Lett.* **115**, 061301 (2015).
 [11] M. J. Baker *et al.*, *J. High Energy Phys.* **12** (2015) 120.
 [12] A. Delgado, A. Martin, and N. Raj, *Phys. Rev. D* **95**, 035002 (2017).
 [13] N. Nagata, H. Otono, and S. Shirai, *Phys. Lett. B* **748**, 24 (2015).
 [14] N. Nagata, H. Otono, and S. Shirai, *Phys. Lett. B* **748**, 24 (2015).
 [15] E. D. Carlson, M. E. Machacek, and L. J. Hall, *Astrophys. J.* **398**, 43 (1992).
 [16] D. J. H. Chung, E. W. Kolb, and A. Riotto, *Phys. Rev. D* **60**, 063504 (1999).
 [17] J. L. Feng, A. Rajaraman, and F. Takayama, *Phys. Rev. Lett.* **91**, 011302 (2003).
 [18] J. L. Feng, H. Tu, and H. B. Yu, *J. Cosmol. Astropart. Phys.* **10** (2008) 043.
 [19] D. E. Kaplan, M. A. Luty, and K. M. Zurek, *Phys. Rev. D* **79**, 115016 (2009).
 [20] L. J. Hall, K. Jedamzik, J. March-Russell, and S. M. West, *J. High Energy Phys.* **03** (2010) 080.
 [21] F. D’Eramo and J. Thaler, *J. High Energy Phys.* **06** (2010) 109.
 [22] Y. Hochberg, E. Kuflik, T. Volansky, and J. G. Wacker, *Phys. Rev. Lett.* **113**, 171301 (2014).
 [23] E. Kuflik, M. Perelstein, Nicolas Rey-Le Lorier, and Y. D. Tsai, *Phys. Rev. Lett.* **116**, 221302 (2016).
 [24] D. Pappadopulo, J. T. Ruderman, and G. Trevisan, *Phys. Rev. D* **94**, 035005 (2016).
 [25] A. Berlin, D. Hooper, and G. Krnjaic, *Phys. Lett. B* **760**, 106 (2016).
 [26] M. Farina, D. Pappadopulo, J. T. Ruderman, and G. Trevisan, *J. High Energy Phys.* **12** (2016) 039.
 [27] J. A. Dror, E. Kuflik, and W. H. Ng, *Phys. Rev. Lett.* **117**, 211801 (2016).
 [28] J. Cline, H. Liu, T. Slatyer, and W. Xue, [arXiv:1702.07716](https://arxiv.org/abs/1702.07716).
 [29] G. R. Farrar and E. W. Kolb, *Phys. Rev. D* **53**, 2990 (1996).
 [30] D. J. H. Chung, G. R. Farrar, and E. W. Kolb, *Phys. Rev. D* **56**, 6096 (1997).
 [31] P. A. R. Ade *et al.* (Planck Collaboration), *Astron. Astrophys.* **594**, A13 (2016).
 [32] T. R. Slatyer, *Phys. Rev. D* **93**, 023527 (2016).
 [33] T. R. Slatyer, *Phys. Rev. D* **93**, 023521 (2016).
 [34] See Supplemental Material at <http://link.aps.org/supplemental/10.1103/PhysRevLett.119.061102> for details about the calculation of thermal correction to the coscattering DM abundance.
 [35] J. Ellis, F. Luo, and K. A. Olive, *J. High Energy Phys.* **09** (2015) 127.
 [36] A. Loeb and M. Zaldarriaga, *Phys. Rev. D* **71**, 103520 (2005).
 [37] T. Bringmann and S. Hofmann, *J. Cosmol. Astropart. Phys.* **04** (2007) 016; T. Bringmann and S. Hofmann, *J. Cosmol. Astropart. Phys.* **03** (2016) E02.
 [38] T. Bringmann, *New J. Phys.* **11**, 105027 (2009).
 [39] H. Goldberg and L. J. Hall, *Phys. Lett. B* **174**, 151 (1986).
 [40] M. J. Strassler and K. M. Zurek, *Phys. Lett. B* **651**, 374 (2007).
 [41] D. P. Finkbeiner and N. Weiner, *Phys. Rev. D* **76**, 083519 (2007).
 [42] M. Pospelov, A. Ritz, and M. B. Voloshin, *Phys. Lett. B* **662**, 53 (2008).
 [43] J. L. Feng and J. Kumar, *Phys. Rev. Lett.* **101**, 231301 (2008).
 [44] N. Arkani-Hamed, D. P. Finkbeiner, T. R. Slatyer, and N. Weiner, *Phys. Rev. D* **79**, 015014 (2009).
 [45] Y. Hochberg, E. Kuflik, H. Murayama, T. Volansky, and J. G. Wacker, *Phys. Rev. Lett.* **115**, 021301 (2015).
 [46] M. A. Buen-Abad, G. Marques-Tavares, and M. Schmaltz, *Phys. Rev. D* **92**, 023531 (2015).
 [47] R. T. D’Agnolo, C. Modino, J. T. Ruderman, and P. J. Wang (to be published).
 [48] J. Chluba and D. Jeong, *Mon. Not. R. Astron. Soc.* **438**, 2065 (2014).

- [49] A. Kogut *et al.*, *J. Cosmol. Astropart. Phys.* **07** (2011) 025.
- [50] M. H. Abitbol, J. Chluba, J. C. Hill, and B. R. Johnson, [arXiv:1705.01534](https://arxiv.org/abs/1705.01534); *Mon. Not. R. Astron. Soc.* (to be published).
- [51] J. D. Bjorken, R. Essig, P. Schuster, and N. Toro, *Phys. Rev. D* **80**, 075018 (2009).
- [52] J. D. Bjorken, S. Ecklund, W. R. Nelson, A. Abashian, C. Church, B. Lu, L. W. Mo, T. A. Nunamaker, and P. Rassmann, *Phys. Rev. D* **38**, 3375 (1988).
- [53] E. M. Riordan *et al.*, *Phys. Rev. Lett.* **59**, 755 (1987).
- [54] M. Davier and H. Nguyen Ngoc, *Phys. Lett. B* **229**, 150 (1989).
- [55] J. P. Lees *et al.* (BABAR Collaboration), *Phys. Rev. Lett.* **113**, 201801 (2014).
- [56] G. G. Raffelt, *Stars as Laboratories for Fundamental Physics* (Chicago University Press, Chicago, 1996), p. 664, .
- [57] A. Burrows and J. M. Lattimer, *Astrophys. J.* **307**, 178 (1986).
- [58] A. Burrows and J. M. Lattimer, *Astrophys. J.* **318**, L63 (1987).
- [59] H. K. Dreiner, C. Hanhart, U. Langenfeld, and D. R. Phillips, *Phys. Rev. D* **68**, 055004 (2003).
- [60] H. K. Dreiner, J. F. Fortin, C. Hanhart, and L. Ubaldi, *Phys. Rev. D* **89**, 105015 (2014).
- [61] J. H. Chang, R. Essig, and S. D. McDermott, *J. High Energy Phys.* **01** (2017) 107.
- [62] C. Boehm, M. J. Dolan, and C. McCabe, *J. Cosmol. Astropart. Phys.* **08** (2013) 041.
- [63] K. N. Abazajian *et al.* (CMB-S4 Collaboration), [arXiv:1610.02743](https://arxiv.org/abs/1610.02743).
- [64] W. Hu and J. Silk, *Phys. Rev. Lett.* **70**, 2661 (1993).
- [65] J. Chluba and R. A. Sunyaev, *Mon. Not. R. Astron. Soc.* **419**, 1294 (2012).
- [66] D. J. Fixsen, E. S. Cheng, J. M. Gales, J. C. Mather, R. A. Shafer, and E. L. Wright, *Astrophys. J.* **473**, 576 (1996).